Chinese J. of Chem. Eng., **8** (2) 108—112 (2000)

Effect of Continuous Phase Viscosity on Membrane Emulsification*

WANG Zhi(王志) and WANG Shichang(王世昌)**
Chemical Engineering Research Center, Tianjin University, Tianjin 300072, China

Volker Schroeder and Helmar Schubert
Institute of Food Process Engineering, Karlsruhe University, D-76128 Karlsruhe, Germany

Abstract Oil-in-water(o/w) emulsions were produced with a membrane emulsification system. The effect of the continuous phase viscosity on the emulsification was studied. The theoretical analyses show that the continuous phase viscosity influences not only the flow field of the continuous phase but also the interfacial tension. The droplet size distribution and disperse phase flux for different continuous phase viscosity were investigated experimentally at constant wall shear stress and constant volume flow rate of the continuous phase respectively.
Keywords membrane emulsification, viscosity, continuous phase

1 INTRODUCTION

Emulsions are dispersions of two or more nearly insoluble phases *e.g.* water and oil. One phase is distributed in form of droplets in the other phase. Emulsions are often prepared as foods, pharmaceuticals and cosmetics. The mainly conventional emulsification systems are rotor-stator-systems and high-pressure homogenizers. In these systems, the droplets of a premix are deformed and disrupted under great stress applied[1].

Membrane emulsification is a new emulsification technology based on the use of a microprous membrane. With this technology, droplets of the disperse phase are produced in a different way from the above conventional technology[2]. Fig. 1 shows the membrane emulsification process for an o/w emulsion. The disperse phase in one side of a hydrophilic microprous membrane is pressurized and permeates through pores of the membrane into the continuous phase flowing along another side of the membrane. Droplets of the disperse phase form at the ends of membrane pores, and detach from the membrane when their diameter reaches to certain value. Emulsifier molecules absorb to the newly formed interfaces to stabilize the emulsion.

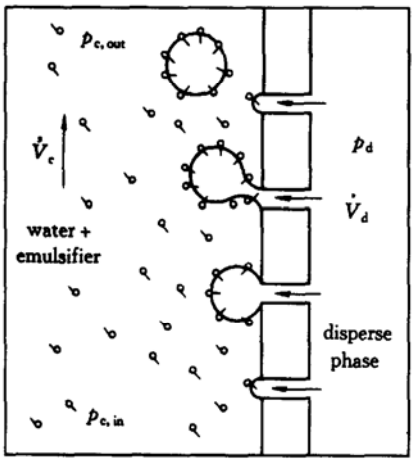

Figure 1 Membrane emulsification process

By using a membrane with a very narrow pore size distribution, one can produce emulsions with a very narrow droplet size distribution[3−5]. Because of the low shear stress at the membrane surface, this method also allows to use shear sensitive ingredients[6]. Moreover with membrane emulsification the energy needed is considerably less than that required by the conventional systems. It is possible to produce o/w, w/o emulsions and even multiple emulsions depending on the membranes used (hydrophilic or lipophilic)[7]. Previous experiments have shown that besides the average pore size of the membrane the transmembrane pressure and the interfacial tension have influence on the result of membrane emulsification[2−6].

In order to prepare a stable emulsion, some substances *e.g.* emulsifiers or stabilizers are usually added in the continuous phase (or disperse phase). Stabilizers change the viscosity of the continuous phase. The purpose of this work is to investigate the effect of the continuous phase viscosity on emulsification with application of a stabilizer.

2 THEORY

2.1 Flux of disperse phase

The flux of disperse phase J_d is determined as follows

Received 1999-01-05, accepted 2000-02-15.
* Supported by the National Natural Science Foundation of China (No. 29506050) and DAAD scholarship.
** To whom correspondence should be addressed.

$$J_d = \frac{\dot{V}_d}{A} \tag{1}$$

It is assumed that J_d obeys Darcy's law, *i.e.*

$$J_d = B\frac{\Delta p_{TM} - \Delta p_\gamma}{\mu_d \Delta L} \tag{2}$$

where B is a factor depending on the membrane structure, Δp_{TM} is the transmembrane pressure and defined as

$$\Delta p_{TM} = p_d - \frac{p_{c,in} + p_{c,out}}{2} \tag{3}$$

Δp_γ is the pressure difference to overcome the capillary effect[8]

$$\Delta p_\gamma = \frac{4\gamma(t)}{d_{dr}} \tag{4}$$

2.2 The forces acting on a droplet

The forces acting on a droplet determine the droplet formation and detachment. These forces can be divided into holding and detaching forces, which hold the droplet on the membrane surface and detach the droplet from the membrane surface respectively. When the detaching forces become higher than the holding forces, the droplet begins to pinch off and breaks away.

The main forces acting on a droplet before its detachment are schematically shown in Fig. 2. They are as follows.

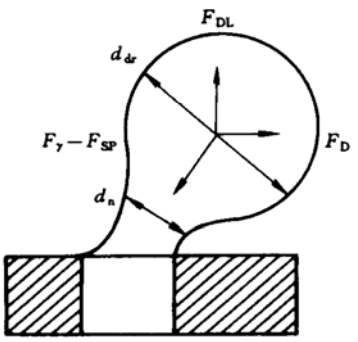

Figure 2 Schematic diagram of forces acting on a droplet

(1) Interfacial tension force

$$F_\gamma = \pi d_n \gamma(t) \tag{5}$$

(2) Static pressure difference force F_{SP}, which is a force due to static pressure difference between the inside and outside of the droplet, *i.e.* between the disperse phase and continuous phase.

$$F_{SP} = (p_d^0 - p_c^0)A_n \tag{6}$$

In quasi-static state

$$p_d^0 - p_c^0 = \Delta p_\gamma \tag{7}$$

From Eqs. (4), (6) and (7) we obtain

$$F_{SP} = \frac{4\gamma(t)}{d_{dr}}\frac{\pi}{4}d_n^2 = F_\gamma \frac{d_n}{d_{dr}} \tag{8}$$

The force F_{SP} is in the same straight line as force F_γ, thus from Eqs. (5) and (8) we obtain

$$F_\gamma - F_{SP} = F_\gamma\left(1 - \frac{d_n}{d_{dr}}\right) = \pi d_n \gamma(t)\left(1 - \frac{d_n}{d_{dr}}\right) \tag{9}$$

Since d_n is always less than d_{dr}, $F_\gamma - F_{SP}$ is positive *i.e.* the direction of $F_\gamma - F_{SP}$ points to the inside of a membrane pore (Fig. 2).

(3) Dynamic lift force F_{DL}, which results from the asymmetric velocity profile of the continuous phase. Rubin gives the following relation for calculating dynamic lift force[9,10]

$$F_{DL} = 0.761\frac{\tau_w^{1.5} d_{dr}^3 \rho_c^{0.5}}{\mu_c} \tag{10}$$

(4) Viscous drag force F_D. It is assumed that the droplets are formed only in the laminar sublayer. For a spherical droplet the viscous drag force can be calculated according to Stokes's equation[11]

$$F_D = 3\pi w_{c,m} d_{dr} \mu_c = \frac{3}{2}\pi \tau_w d_{dr}^2 \tag{11}$$

Among these forces, F_γ is a holding force, while F_{SP}, F_{DL} and F_D are detaching forces. Increase in $F_\gamma - F_{SP}$ will increase the diameter of droplets at detachment, while increase in F_{DL} and F_D will decrease the diameter of droplets at detachment. The other forces like the inertial force, buoyancy force and gravity force are negligible in our calculation[12].

2.3 The probable influence of continuous phase viscosity

2.3.1 *Influence on wall shear stress*

The relationship of the continuous phase viscosity μ_c and the wall shear stress τ_w is[12]

$$\tau_w = 8\frac{\mu_c \bar{u}_c}{D_i} = 32\frac{\mu_c \dot{V}_c}{D_i^3} \quad \text{(for laminar flow)} \tag{12}$$

and

$$\tau_w = 0.03955\frac{\mu_c^{0.25}\rho_c^{0.75}\bar{u}_c^{1.75}}{D_i^{0.25}} = 0.003496\frac{\mu_c^{0.25}\rho_c^{0.75}\dot{V}_c^{1.75}}{\pi^{1.75}D_i^{3.75}} \quad \text{(for turbulent flow)} \tag{13}$$

From Eqs. (12) and (13), τ_w is proportional to μ_c for laminar flow and to $\mu_c^{0.25}$ for turbulent flow. Therefore, the continuous phase viscosity will affect the forces F_D and F_{DL} acting on the droplet. Eqs. (12) and (13) indicate that when μ_c varies, τ_w can be kept constant by changing volume flow rate of continuous phase $\dot{V}_c$.

2.3.2 *Influence on interfacial tension*

As time goes on, more and more emulsifier molecules adsorb to the newly formed interface between oil and water to cause a reduction of the interfacial tension $\gamma(t)$. Hence $\gamma(t)$ is a function of interface age t. Three steps must be considered in adsorption of emulsifier molecules[13]: (1) solution of emulsifier micellae; (2) transport of emulsifier molecules from the aqueous bulk phase to the interface; (3) adsorption of emulsifier molecules at interface *i.e.* the transfer of the molecules from the dissolved state to the adsorbed state. If the oil droplets are within the laminar sublayer, the transport of emulsifier molecules to the interface is by diffusion. The diffusion coefficient can be described with the following Stokes-Einstein equation[14]

$$D_e = \frac{kT}{a\mu_c} \tag{14}$$

According to this equation the diffusion coefficient of emulsifier is inversely proportional to the continuous phase viscosity μ_c. It means that with increasing μ_c the rate of reduction of $\gamma(t)$ decreases due to decreasing diffusion coefficient of emulsifier.

3 EXPERIMENTAL

3.1 Materials

In this work only o/w emulsions were prepared. Purified vegetable oil was used as the disperse phase. The continuous phase consists of deionized water and polyethylene glycol (PEG) 20000, which is often used as a stabilizer of emulsions. The greater the PEG concentration, the higher the viscosity of the continuous phase. By changing PEG concentration we obtain continuous phases with different viscosity. The viscosity was measured with a Controlled Stress Rheometer (Carri-Med Germany Ltd., Duesseldorf). Sodium dodecyl sulfate (SDS) was used as emulsifier in the continuous phases.

3.2 Membranes

The membranes used are aluminium oxide (α-Al_2O_3) membrane tubes (Membranflow, Germany). The inner diameter of the membrane tube is 7 mm, and the effective area of membrane surface is about 0.005 m^2.

3.3 Apparatus

The membrane emulsification apparatus used in this study is shown in Fig. 3. The continuous phase or emulsion was circulated through the inner side of the membrane tube. The disperse phase was stored in a container, and was pressurized with compressed air. Through a pipe the oil reaches the outside of the membrane tube. The oil container was put on an electric balance in order to determine the mass of oil added in the continuous phase. The oil flux J_d was calculated from this mass.

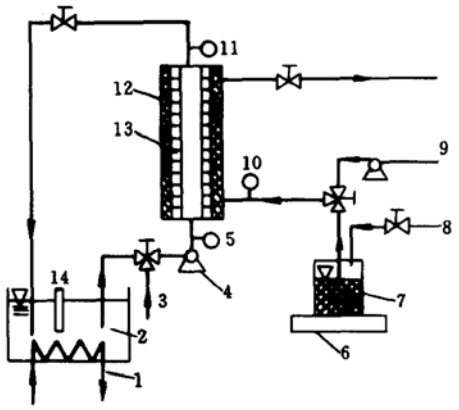

Figure 3 Membrane emulsification apparatus
1—cooling system; 2—water with stabilizer and emulsifier; 3,9—cleaning solution; 4—pump; 5,10,11—manometer; 6—electric balance; 7—oil; 8—compressed air; 12—membrane module; 13—membrane; 14—thermometer

3.4 Measurement of emulsion properties

The average droplet diameter and the droplet size distribution of emulsions were measured by means of a laser-scattering particle analyzer (Master Sizer X, Malvern Instruments Ltd., Herrenbeg). The average droplet diameter was expressed in sauter diameter $d_{3,2}$. The span of the droplet distribution was defined as follows

$$\frac{x_{3,90} - x_{3,10}}{x_{3,50}} \tag{15}$$

where $x_{3,z}$ (z=10, 50, 90) is a droplet diameter, which means z% volume of the disperse phase form droplets with diameter not larger than $x_{3,z}$.

4 RESULTS AND DISCUSSIONS

4.1 Effect of continuous phase viscosity on average droplet diameter and span of the droplet size distribution

Fig. 4 shows the relationship between the average droplet diameter $d_{3,2}$ and the continuous phase viscosity μ_c under different transmembrane pressure drop Δp_{TM} when the wall shear stress τ_w is constant. For every Δp_{TM}, $d_{3,2}$ increases with increasing μ_c. This is because that when τ_w is constant, with increasing μ_c, F_{DL} decreases [see Eq. (10)], and $F_\gamma - F_{SP}$ increases due to the decrease of reduction rate of $\gamma(t)$ [see Eq. (9)]. Thus, the diameter of droplets at detachment increases. This leads to the increase of $d_{3,2}$.

Moreover it is possible that the droplets coalesce due to insufficient adsorption of the emulsifier molecules on the interface. Besides, an osmotic pressure gradient between the bulk phase and the gap of two droplets will form when the PEG-molecules can not reach the liquid film between the droplets. In this

case the water will flow out from the gap and therefore diminish the stabilized film between droplets. If a critical film thickness is reached, the droplets will coalesce. These will also lead to the increase of $d_{3,2}$ with increasing μ_c.

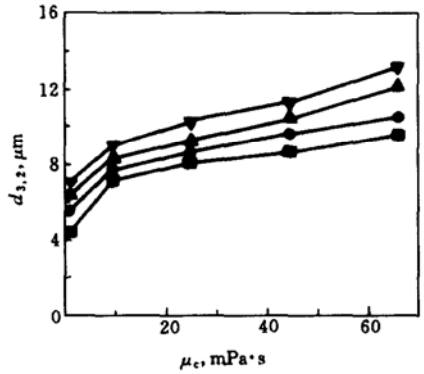

Figure 4 Average droplet diameter $d_{3,2}$ *versus* continuous phase viscosity μ_c under different transmembrane pressure Δp_{TM}
(emulsifier: 2% SDS; average pore diameter of the membrane: 0.5 μm; operating temperature: 25℃; τ_w=33 Pa)
$\Delta p_{TM} \times 10^{-5}$, Pa: ■ 1.5; ● 2.0; ▲ 2.5; ▼ 3.0

Fig. 5 shows the relationship between $d_{3,2}$ and μ_c under a fixed Δp_{TM} when the volume flow rate of continuous phase $\dot{V}_c$ is constant. With increasing μ_c, $d_{3,2}$ increases till $\mu_c \approx 10$ mPa·s and then decreases. From Eqs. (12) and (13), τ_w will increase with increasing μ_c when $\dot{V}_c$ is constant. According to Ref. [12] the increase of τ_w will lead to a decrease in $d_{3,2}$. Therefore, with increasing μ_c the change of $d_{3,2}$ in Fig. 5 should result from the increase of $d_{3,2}$ due to the reasons mentioned above in the discussion on Fig. 4, and the decrease of $d_{3,2}$ due to the increase of τ_w.

In the scope of this experimental work, the span of the droplet size distribution is independent of the continuous phase viscosity. It varies between 1.2 and 1.6.

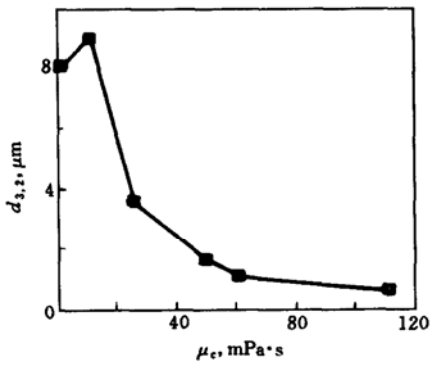

Figure 5 Average droplet diameter $d_{3,2}$ *versus* continuous phase viscosity μ_c
(emulsifier: 2% SDS; average pore diameter of the membrane: 0.8 μm; operating temperature: 25℃; Δp_{TM}=2.0×10^5 Pa; $\dot{V}_c$ = 0.45m^3·h^{-1})

4.2 Effect of continuous phase viscosity on disperse phase flux

Fig. 6 shows the relationship between the disperse phase flux J_d and μ_c for different Δp_{TM} when τ_w is constant. With increasing μ_c, J_d decreases slightly when $\mu_c < 10$ mPa·s, and then keeps approximately constant. This is because of two tendencies, one is the decrease in Δp_γ due to the increase of d_{dr} with increasing μ_c (see 4.1), and the other is the increase in Δp_γ due to the decrease of reduction rate of $\gamma(t)$ with increasing μ_c.

Fig. 7 shows the relationship between J_d and μ_c when $\dot{V}_c$ is constant. In this figure, with increasing μ_c, J_d increases when μ_c is less than about 60 mPa·s, and then keeps approximately constant. This can also be interpreted easily by the varying of τ_w, d_{dr} and $\gamma(t)$ with μ_c. The varying of J_d with τ_w has been studied by our previous work[12].

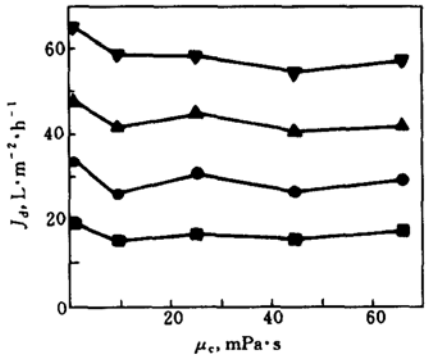

Figure 6 Disperse phase flux J_d *versus* continuous phase viscosity μ_c under different transmembrane pressure Δp_{TM}
(emulsifier: 2% SDS; average pore diameter of the membrane: 0.5 μm; operating temperature: 25℃; τ_w=33 Pa)
$\Delta p_{TM} \times 10^{-5}$, Pa: ■ 1.5; ● 2.0; ▲ 2.5; ▼ 3.0

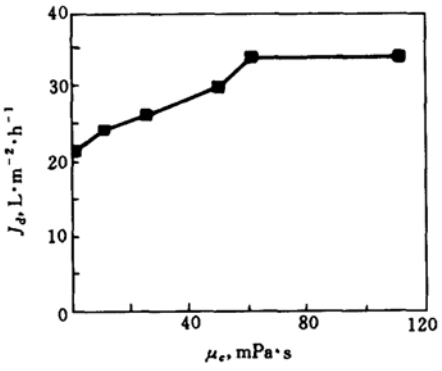

Figure 7 Disperse phase flux J_d *versus* continuous phase viscosity μ_c
(emulsifier: 2% SDS; average pore diameter of the membrane: 0.5 μm; operating temperature: 25℃; Δp_{TM} = 2.0 × 10^5 Pa; $\dot{V}_c$=0.45 m^3·h^{-1})

5 CONCLUSIONS

(1) For membrane emulsification, the viscosity of continuous phase influences the wall shear stress and the diffusion of emulsifier molecules, and therefore influences the emulsification.

(2) For constant wall shear stress with increasing of the continuous phase viscosity, the average droplet diameter of the emulsion increases; the disperse phase flux decreases slightly when the viscosity is less than 10 mPa·s and then keeps constant.

(3) For constant volume flow rate of the continuous phase, with increasing of the continuous phase viscosity, the average droplet diameter increases when the viscosity is less than 10 mPa·s, and then decreases; the disperse phase flux increases when the viscosity is less than 60 mPa·s, and then keeps constant.

NOMENCLATURE

A	area of membrane surface, m^2
A_n	cross-sectional area of the droplet neck, m^2
a	length of emulsifier molecule, m
B	factor depending on membrane pore characteristics [Eq. (2)].
D_e	diffusion coefficient of emulsifier, $m^2 \cdot s^{-1}$
D_i	inner diameter of membrane tube, mm
d_{dr}	diameter of oil droplet, μm
d_n	diameter of the droplet neck, μm
$d_{3,2}$	average droplet diameter of emulsion, μm
F_D	viscous drag force, N
F_{DL}	dynamic lift force, N
F_{SP}	Static pressure difference force, N
F_γ	Interfacial tension force, N
J_d	disperse phase flux, $L \cdot m^{-2} \cdot h^{-1}$
k	Boltzmann's constant, $J \cdot K^{-1}$
ΔL	membrane thickness, m
$p_{c,in}$	pressure of continuous phase at the module inlet, Pa
$p_{c,out}$	pressure of continuous phase at the module outlet, Pa
p_d	pressure of disperse phase, Pa
p_c^0	pressure of continuous phase on membrane surface, Pa
p_d^0	pressure of disperse phase on membrane surface, Pa
Δp_{TM}	transmembrane pressure, Pa
Δp_γ	pressure difference to overcome the capillary effect, Pa
T	absolute temperature, K
$\overline{u}_c$	average velocity of continuous phase in membrane tube, $m \cdot s^{-1}$
$\dot{V}_c$	volume flow rate of continuous phase, $m^3 \cdot h^{-1}$
$\dot{V}_d$	volume permeation rate of disperse phase, $m^3 \cdot h^{-1}$
$w_{c,m}$	average velocity of continuous phase flowing past the surface of forming droplet, $m \cdot s^{-1}$
$x_{3,z}$	droplet diameter, which means z% volume of the disperse phase form droplets with diameter not larger than $x_{3,z}$, μm
$\gamma(t)$	interfacial tension, $N \cdot m^{-1}$
μ_c	viscosity of continuous phase, mPa·s
μ_d	viscosity of disperse phase, mPa·s
ρ_c	density of continuous phase, $kg \cdot m^{-3}$
τ_w	wall shear stress, Pa

REFERENCES

1 Karbstein, H., Schubert, H., *Chem. Eng. and Proc.*, **34**, 205 (1995).
2 Katoh, R., Asano, Y., Furuya, A., Sotoyama, K., Tomita, M., *J. Membrane Sci.*, **113**, 131 (1996).
3 Kandori, K., Kishi, K., Ishikawa, T., *Colloids Surf. A*, **55**, 73 (1991).
4 Kandori, K., Kishi, K., Ishikawa, T., *Colloids Surf. B*, **61**, 269 (1991).
5 Schröder, V., Wang, Z., Schubert, H., Proc. 3rd Inter. Symp., Euromembrane '97, Kemperman, A. J. B., Koops G. H., eds., University of Twente, The Netherlands, 439 (1997).
6 Schröder, V., Schubert, H., Proceedings of the ECCE-1, Vol. 4, Florence, Italy, 2491,(1997).
7 Kandori, K., In: Food Processing: Recent Development, Gaonkar, A. G., ed., Elsevier Science B. V, The Netherlands, 113 (1995).
8 Adamson, A. W., Physical Chemistry of Surfaces, 5th ed., John Wiley & Sons Inc., New York, 5 (1990).
9 Rubin, G., Ph. D. Thesis, University Karlsruhe, Karlsruhe (1977).
10 Stölting, M., *Chemie Ingenieur Technik*, **52** (7), 817 (1980).
11 Scheel, G. F., Meister, B. J., *AIChE J.*, **145** (1), 9 (1968).
12 Wang, Zh., Wang, S. Ch., Schroeder, V., Schubert, H., *Journal of Chemical Industry and Engineering (China) (in Chinese)*, **50** (4), 505 (1999).
13 Stang, M., Karbstein, H., Schubert, H., *Chem. Eng. and Proc.*, **33**, 307 (1994).
14 Menon, N., Nagel, S. R., Venerus, D. C., *Phys. Rev. Lett.*, **73**, 963 (1994).